

# Improvement of the Rheological Behavior of Viscoelastic Surfactant Fracturing Fluids by Metallic-Type Nanoparticles

Saber Mohammadi,\* Alimohammad Hemmat, Hamidreza Afifi, and Fatemeh Mahmoudi Alemi

Cite This: *ACS Omega* 2024, 9, 28676–28690

Read Online

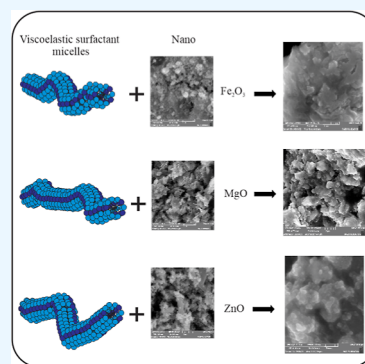
ACCESS |

Metrics & More

Article Recommendations

Supporting Information

**ABSTRACT:** The use of nanotechnology in the field of acidizing, particularly in fracturing fluids, has garnered significant attention over the past decade. Viscoelastic surfactants (VESs) are utilized as one of the most effective fracturing fluids, possessing both elasticity and viscosity properties. These fluids are crucial additives in acidizing packages, enhancing their performance. However, various factors, such as salinity, temperature, pressure, and concentration, can sometimes weaken the efficacy of these fluids. To address this, the integration of nanoparticles has been explored to improve fluid retention in reservoirs and enhance the efficiency. This study focuses on investigating the impact of the main metallic-type nanoparticles on the rheological behavior of VES fluids. Iron oxide, magnesium oxide, and zinc oxide nanoparticles were utilized, and the microscopic-scale rheological behavior of the fluids was thoroughly evaluated. The highest performance for enhancing fluid gelation, stability, and rheological characteristics of VES fluids was found for Fe<sub>2</sub>O<sub>3</sub> nanoparticles at an optimum concentration of 500 ppm. At this concentration and shear rate of 100 s<sup>-1</sup>, the viscosity of the fluid reached 169.61 cP. For iron oxide nanoparticles at a concentration of 500 ppm, by increasing the temperature from 25 to 85 °C, the gelation state of the fluid increased from 7 h and 50 min to 17 h and 45 min. This improvement is attributed to their high surface area and the increased density of entanglement points within the micelles, leading to a more interconnected structure with enhanced viscoelastic properties. Furthermore, iron oxide nanoparticles significantly enhance gelation by physically connecting the micelles, thereby improving stability and structure. The absorption of surfactant molecules by the nanoparticles additionally contributes to micelle reconstruction and shape alteration. The presence of iron oxide nanoparticles helps maintain the gel structure even at elevated temperatures, preventing rapid viscosity decrease. Our findings may provide new insights for development of high-performance, economical, and environment-friendly fracturing fluids used in well stimulation operations.



## 1. INTRODUCTION

Initially, oil-based fracturing fluid was used to create fractures in the reservoir, but due to environmental concerns, it quickly lost its use and was replaced by water-based fracturing fluids.<sup>1,2</sup> These types of fluids are very cheap and have excellent applications, but in high-temperature areas, there is a lack of improvement in performance, and the efficiency of the fluid decreases. In recent decades, methods of matrix acidizing and fracture treatment have been used to improve the well performance, generally using water- and acid-soluble polymers.<sup>3,4</sup>

To reduce the amount of leakage during acid injection into fractures, fluids with high viscosity are needed.<sup>5</sup> Various chemicals have been used to increase the viscosity of the fluid, but in general, this system can be divided into two categories depending on the viscosity agent: (1) polymer-based fluids and (2) surfactant-based fluids.<sup>6,7</sup> But, for two reasons, polymers were less useful: (1) it is uneconomical to use polymers in high concentrations to achieve higher viscosity and (2) polymer residues formed in the formation and damaged the reservoir. As a result, the use of viscoelastic surfactants (VESs) has become more popular than the polymer-based fluids.<sup>8–10</sup> Therefore, the use of surfactant-based fluids such as VESs was

considered instead of polymer-based fluids because they have suitable rheological properties and are compatible with various KCl, CaBr<sub>2</sub>, and CaCl<sub>2</sub> salts, as well as the crude oil.<sup>11</sup> Moreover, the use of this type of fluid does not cause damage to the formation. Among the other advantages that have favored the use of VESs is that the presence of hydrophobic salts in the environment causes strong binding in the micelles of surfactants and their rapid growth.<sup>12–14</sup>

Surfactants decompose at high temperatures and cannot fix the foam system.<sup>15–18</sup> The addition of VESs to surfactants can improve their performance and stability. The addition of VESs improves the stability of the surfactant due to the increase in the viscosity of the liquid and the increase in the lamella thickness.<sup>19–21</sup> The use of fluid systems based on the VES has attracted much attention since the mid-1980s. The use of VESs

Received: March 28, 2024

Revised: June 10, 2024

Accepted: June 12, 2024

Published: June 21, 2024



increases fluid viscosity through the unique arrangement of surfactants in a long or worm-like micelle structure.<sup>22</sup> These types of structures tend to be very sensitive to ion concentration and fluid temperature.<sup>23</sup>

VESs have an advantage that other fluids do not have. They cause the least damage to the formation and have high reverse permeability, high ability to break gels, low frictional pressure, and ease of manufacturing.<sup>24,25</sup> However, VES materials are less stable at high temperatures and have low shear rates. In general, VESs have smaller molecules with molecular weights below 1000, and reactions such as repulsion and attraction occur between the surfactant and solvent; it can cause the surfactant itself to assemble into colloidal structures such as worm-like micelles.<sup>26,27</sup> When the concentration of the surfactant in the VES is higher than its critical concentration, the worm-like micelles combine with each other and cause the liquid to be difficult to move, resulting in an elastic and viscous behavior in the liquid.<sup>28</sup> However, the use of this type of liquid is limited to the temperature. They usually show poor behavior in environments above 200 °F.<sup>12,29</sup> Another limitation of using VES liquids is that since a large volume has penetrated into the matrix, they must be removed or purged from the matrix after the treatment process.<sup>30</sup>

One of the advantages of the VES fluids is that no filter cake forms on the reservoir wall. Therefore, these types of fluids can easily penetrate into the matrix. VES fluids can easily leak into the matrix, and control of the fluid leakage depends on the viscosity of the fluid itself rather than the reservoir wall. Therefore, it is more appropriate to use VESs in reservoirs where the permeability is less than 800–1200 md and preferably less than 400 md.<sup>31,32</sup>

Polymers are among the fluids used in fracturing applications. Polymers are recommended for high-temperature applications due to their higher thermal stability. However, they can cause damage to the formation due to their high molecular weight.<sup>21,33</sup> Therefore, the VES is used as an alternative because it has a lower molecular weight and is less likely to damage the formation. In general, these materials have low rheological and thermal stability, but by increasing the VES concentration up to a viscosity of 50 to 100 cP and a shear rate of 170 s<sup>-1</sup>, this issue is largely solved. The micellization process in the VES depends on the electrostatic interaction between the chemical species in the solution.<sup>34,35</sup> In general, increasing the counterion concentration leads to screening of the charged head groups in the VES and decreases the repulsion between the surfactant heads. Addition of nanoparticles increases the apparent viscosity without changing the length of the micelles. The interaction between the VES and nanoparticles is defined as a quasi-cross-surfactant system, where the nanoparticles become compressing compounds in the VES micelle network. The use of nanoparticles with the opposite charge causes the adsorption of the surfactant on the surface of nanoparticles through the head groups to interact and form a bilayer surfactant structure, which shows the synergistic effect and the increase of the apparent viscosity of the system.<sup>17,36</sup> Several studies show that the critical micelle concentration (CMC) decreases with the increase of ion concentration in the environment.<sup>37,38</sup> For example, the addition of CaCl<sub>2</sub> and CaBr<sub>2</sub> salts at concentrations ranging from 10 to 23 wt % can be seen to decrease the CMC concentration in VESs. As the concentration of other ions increases, the shielding in the charged surfactant wedges also increases and the repulsion between the surfactant heads

decreases.<sup>28,39</sup> This leads to the micellization of a stronger network. Moreover, the addition of nanoparticles such as MgO, ZnO, and SiO<sub>2</sub> to this type of material can increase the apparent viscosity and thermal stability of the VES-based fluids.<sup>19,40</sup> Recent studies show that the addition of this type of nanoparticles could maintain the apparent viscosity of the fluid at a value of 200 cP for 80 min at a temperature of 250 °F, while the viscosity decreased to 40 cP in the absence of nanoparticles.<sup>30</sup> It has also been shown that the use of nanomaterials having a charge opposite to the surfactants enhances the absorption phenomenon to the point of forming a bilayer surfactant structure, leading to an increase in the viscosity of the liquid.<sup>41–44</sup>

Iron oxide nanoparticles are used as an additive to enhance the electromagnetic absorption properties. In addition, it has been studied how to optimize the heating process and increase oil recovery. When nanoparticles are used in the reservoir, five phenomena occur: 1 absorption, 2 disposal, 3 blocking, 4 transport, and 5 accumulation.<sup>43,45</sup> The first three phenomena occur between the fluid and the rock, and the next two occur between the nanoparticles themselves. When two fluids are in contact, there is an interaction between the fluids. Thus, when nanoparticles are in a fluid that is in contact with another fluid, there is a possibility that they will shift into another fluid, which is called a diffusion phenomenon.<sup>46,47</sup> The important thing to note here is that diffusion occurs when there is a difference in the concentration between the two liquids. If this kind of behavior of nanoparticles is used in VES materials, it will increase the efficiency of the oil in the matrix. This is because they can be associated with the oil fluid and reduce the heat transfer loss since the emission of nanoparticles is directly transferred as heat energy to the oil phase during emission.<sup>48,49</sup>

For the past decade, nanotechnology has played a crucial role in enhancing the performance of VES fracturing fluids. Compared with traditional materials, nanomaterials offer improved physical and chemical properties. In VES solutions, stable electrostatic bridges form between nanoparticles and surfactant micelles, which modify the rheology and microstructural behavior of the solution. Nanoparticles enhance micellar entanglements by increasing micellar length, ultimately improving VES solution viscoelasticity and viscosity.<sup>22,46</sup> The viscosity of the VES fluid tends to deteriorate as temperatures increase, limiting its applications in certain formations. Researchers have tirelessly worked to improve micelle strengths, especially at elevated shear temperature, through the use of nanoparticles with VES fracturing fluids.<sup>31,50</sup>

Due to the specific surface area and small size of the nanoparticles, they demonstrate strong absorption ability and suspension stability in the VES solutions. The amphiphilic nature of the surfactants results in partition at the solid–liquid interface, a behavior that is influenced by the presence of nanoparticles. The surface chemistry of amphiphilic and the nature of their self-assembly are determined by the interaction between the head and tail groups. Nanoparticles with a strong affinity for the surfactant head induce electrostatic and/or van der Waals interactions, causing the surfactant to adsorb on the surface of nanoparticles in a head-on fashion. The addition of nanoparticles leads to improved plateau modulus, relaxation time, and zero shear viscosity in nanoparticles–VES fluids.<sup>37,44,51</sup>

In the past, the addition of nanoparticles to the VES solution to improve its performance was considered to be detrimental

to production because these particles act as pore blockers, thereby affecting the permeability and efficiency of the reservoirs.<sup>52,53</sup> However, it has been found that selected particles of nano size and less than 100 nm can improve the performance of VES fluids. Since the molecular weight of the surfactant in VES materials is less than 500, the particle size should be less than 100 nm to avoid damaging the formation. Recently, it was discovered that selected nanoparticles exhibiting pyroelectric behavior can improve the quasi-bonded properties of micelles in VES materials.<sup>54,55</sup> In general, pyroelectric particles show an increase in the electrostatic charges on their crystal surface when heated. The use of this type of particle causes the quasi-bonding properties of the micelles to improve with increasing temperature, and the micelles exhibit more internal communication.<sup>37,54</sup>

According to the described literature survey, further detailed studies should be conducted to investigate the beneficial effects of metallic-type nanoparticles on enhancing the performance of fracturing fluids, particularly VESs. To the best of our knowledge, the beneficial effects of different metallic-based nanoparticles on improvement of the performance of VES fracturing fluids have not been comprehensively studied. In addition, there is a lack of mechanistic investigations to understand the mechanisms of nanoparticles–VES fluids. Thus, further experimental studies should be conducted to fill the mentioned gaps. This study aims to examine the impact of the main metallic-based nanoparticles, magnesium oxide, zinc oxide, and iron oxide, on enhancing the rheological behavior of viscoelastic fracturing fluids. Generally, the addition of nanoparticles to fracturing fluid has frequently demonstrated improvements in their performance. However, it is important to note that each nanoparticle operates via a distinct functional mechanism under identical conditions. Therefore, this study endeavors to ascertain the behavior of micelles in relation to nanoparticles and the maintenance of fluid gelation at the microscopic scale and various temperature conditions. As well, the effects of influencing parameters such as surfactant concentration and type of nanoparticles on VES rheological behavior are studied in detail.

## 2. MATERIALS AND METHODS

**2.1. Fluids and Materials.** To conduct the experiments, sodium dodecyl sulfate (SDS) was used as a surfactant to prepare the original solution (Table 1). Distilled water was also used as the main phase of the solutions. CaCl<sub>2</sub> salt and VES2000, obtained from *Energy Chemical Co. Semnan*, were used in these experiments to make the gel phase.

After calculating the optimal concentrations of the surfactant and VES for the initial preparation of the solution, three types

of nanoparticles (Fe<sub>2</sub>O<sub>3</sub>, MgO, and ZnO) were synthesized and used in designed tests to improve the rheological performance of the solutions. The studied nanoparticles were synthesized by the chemical precipitation method.<sup>55–58</sup> As the synthesis of the nanoparticles is out of scope of this work, detailed descriptions about the methods of preparation of nanoparticles can be found in the mentioned references. Essentially, this article intends to focus on the application and effects of the nanoparticles in rheological properties of VES solutions. *The synthesized nanostructures were fully characterized by X-ray diffraction (XRD, PANalytical X'Pert PRO, λ = 0.15406 nm), field emission scanning electron microscopy (FESEM, FEI Nova NanoSEM 450), and Brunauer–Emmett–Teller (BET, Belsorp mini II, Microtrac Bel Corp) techniques.*

The M3600 automatic rheometer was used to perform the rheology tests, which has the ability to adjust the temperature, shear rate, and shear stress. Additionally, an IKA RW-20 electric stirrer was used to prepare the solutions. Lastly, a *Bain-marie* bath was used to increase the temperature of the solutions to 85 °C.

**2.2. Foam Stability Test Methods.** Foam stability is closely related to its texture and structure. Typically, there are two primary methods used to evaluate the stability of the foam solutions. The first method, known as half-life, involves creating a surfactant solution and injecting gas into it until the foam reaches its maximum height in a cylinder. The time it takes for the height of the foam to reach half of its original height is referred to as the foam's half-life ( $t_{1/2}$ ). A longer half-life indicates a greater foam stability. The second method involves calculating  $R_5$  time. Once the gas injection stops and the foam reaches its maximum height, its height is measured 5 min later.<sup>59,60</sup> Using a specific formula,  $R_5$  can then be determined as follows

$$R_5 = \frac{h_2}{h_1} \cdot 100 \quad (1)$$

where  $h_2$  is the height of the foam after 5 min and  $h_1$  is the initial height of the foam. The higher the amount of  $R_5$ , the more stable the foam solution.

**2.3. Experimental Procedures Protocol.** **2.3.1. Finding the Optimum Surfactant Concentration.** The most stable foam is achieved by optimizing the CMC of the surfactant. To determine this value, solutions of the anionic SDS surfactant were prepared by using distilled water as the base phase. Various concentrations of SDS (0.10, 0.20, 0.50, 0.75, 1.00, and 1.50 wt %) were prepared, and nitrogen gas at a pressure of 400 psi was injected to reach the maximum foam height. The process of foam height reduction over time was then monitored upon cessation of gas injection, and the parameters of half-life and  $R_5$  were calculated. Figure 1 depicts the schematic of the setup used for determination of the foam stability.

**2.3.2. Determining the Optimal VES Concentration.** To create the gel phase, the optimal amount of SDS obtained from the previous step and 23.3 g of CaCl<sub>2</sub> salt, which is equivalent to 15% hydrochloric acid, were added, following chemical calculations to produce a 100 mL solution. The appropriate concentration of the VES was then determined and added to the solution to achieve the highest viscosity at both ambient temperature and 85 °C. To accomplish this, experiments were conducted based on two VES concentrations of 6 and 7.5% wt. For each concentration, two solutions were prepared in

**Table 1. Physical and Chemical Properties of SDS**

specification	value
formula	C <sub>12</sub> H <sub>25</sub> O <sub>4</sub> S·Na
molecular weight (g/mol)	288.38
physical state	powder
color	white
melting point (°C)	204
flash point (°C)	170
pH	9.1
density (g/cm <sup>3</sup> )	0.370
bulk density (kg/m <sup>3</sup> )	<400 kg/m <sup>3</sup>

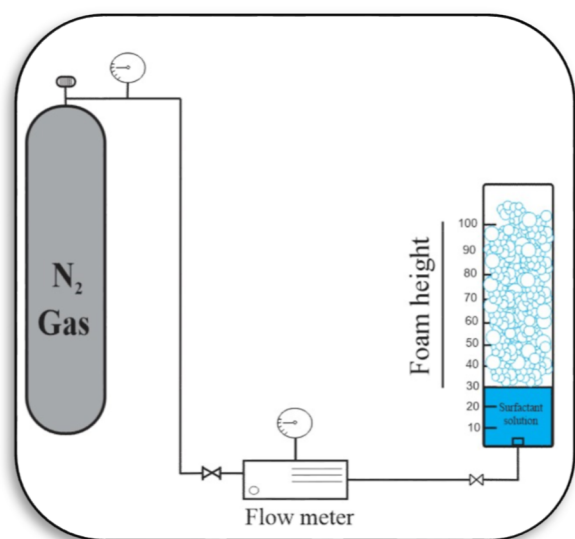


**Figure 1.** Schematic of the setup used for determination of the foam stability.

accordance with Table 2. Finally, using a *grace M3600* machine and a constant shear rate of  $100 \text{ s}^{-1}$ , the viscosity values of the solutions were measured at ambient temperature and  $85 \text{ }^\circ\text{C}$ .

**Table 2.** Preparation of Solutions for Tests to Determine the Optimal Amount of the VES Concentration

solution number	distilled water volume (mL)	CaCl <sub>2</sub> salt (g)	SDS (% wt)	VES (% wt)
1	100	23.3	1.0	6.0
2	100	23.3	1.0	7.5
3	100	23.3		7.5

**2.3.3. Effect of Metallic Nanoparticles on Improving the Rheological Performance of Gel Solution.** After determining the optimal VES concentration, the effect of adding three types of nanoparticles, MgO, ZnO, and Fe<sub>2</sub>O<sub>3</sub>, on the rheological performance of the gel solution was assessed. To this end, 10 solutions at varying concentrations of 500, 1000, and 2000 ppm were prepared for each nanoparticle separately. The rheological behavior of the prepared solutions was evaluated in the following steps. During the first step, rheological behavior was evaluated for each solution at ambient temperature, with shear rates ranging from  $0.1$  to  $1000 \text{ s}^{-1}$ . During the second

step, changes in fluid rheological behavior at  $85 \text{ }^\circ\text{C}$  were investigated with a constant shear rate of  $100 \text{ s}^{-1}$  to analyze the behavior of the mixture obtained across a range of temperatures.

**2.3.4. Effect of Nanoparticles on Improving the Carrying Capacity of Bentonite Particles.** In this step, a 10 mL cylinder was used to pour 10 mL of each solution made from the previous step, and then, 0.1 g of bentonite was added to the solution. To test the ability to carry the particles, the duration of carrying bentonite by the solution was measured in two different parts. In the first part, the time it takes for all of the bentonite added to the solution to enter the solution was measured. In the second part, the time it took for the bentonite to settle at the bottom of the cylinder was evaluated. It should be noted that 10 solutions were made in this test. A VES base free of nanoparticle solution and nine VES solutions with nanoparticles in concentrations of 500, 1000, and 2000 were prepared.

**2.3.5. Investigating the Preservation of the Gelation State in the Presence of Nanoparticles.** At this stage, the solution preservation test is evaluated. For this purpose, a total of 10 solutions are used. The basic solution includes VES, SDS, distilled water, and CaCl<sub>2</sub> salt. Additionally, 9 other solutions are prepared by adding nanoparticles of MgO, ZnO, and Fe<sub>2</sub>O<sub>3</sub> at concentrations of 500, 1000, and 2000 ppm. After the gels were formed, the time taken for each solution to lose its gel state and become a flowing liquid was measured at two ambient temperatures and  $85 \text{ }^\circ\text{C}$ .

**2.3.6. Effect of Nanoparticles on Changes in Storage Modulus ( $G'$ ) and Loss Modulus ( $G''$ ).** One method for studying the microstructure of fracture fluid involves using a dynamic oscillatory measurement. This method measures the values of the storage modulus ( $G'$ ) and loss modulus ( $G''$ ). The storage modulus provides information about the energy stored in the elastic structure of the sample, while the loss modulus parameter indicates the viscous part or the energy dissipated in the sample. In this section, the changes in the parameters ( $G'$ ) and ( $G''$ ) were evaluated in four solution samples, which had the best rheology in previous stages, both with and without nanoparticles. It is important to note that the effect of temperature was accounted for in this test. The *Anton Paar* rheometer (model *MCR501*) was used for the measurement of  $G'$  and  $G''$ . This rheometer allows us to accurately apply torques from  $0.01 \mu\text{N}\cdot\text{m}$  to  $300 \text{ mN}\cdot\text{m}$  with a resolution of  $0.1 \text{ nN}\cdot\text{m}$  and normal forces from  $0.01$  to  $50 \text{ N}$  with a resolution of  $0.002 \text{ N}$ . It is equipped with a pressure cell that allows measurements under pressure up to  $150 \text{ bar}$ . Temper-

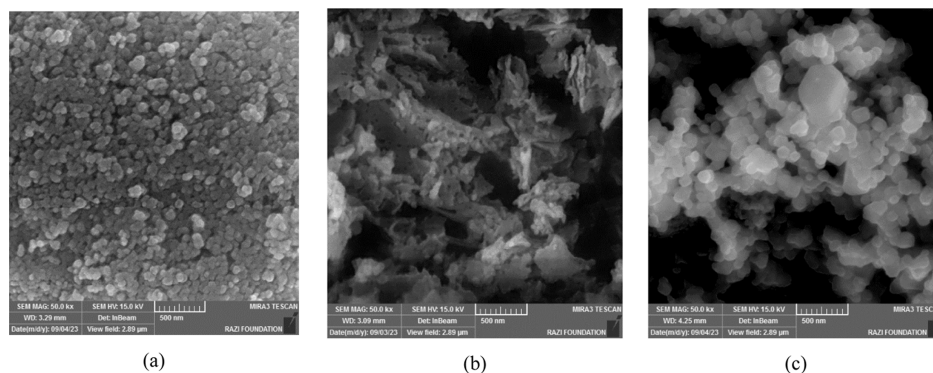


**Figure 2.** FESEM images of pure metallic nanoparticles: (a) Fe<sub>2</sub>O<sub>3</sub> nanoparticles, (b) MgO nanoparticles, and (c) ZnO nanoparticles.

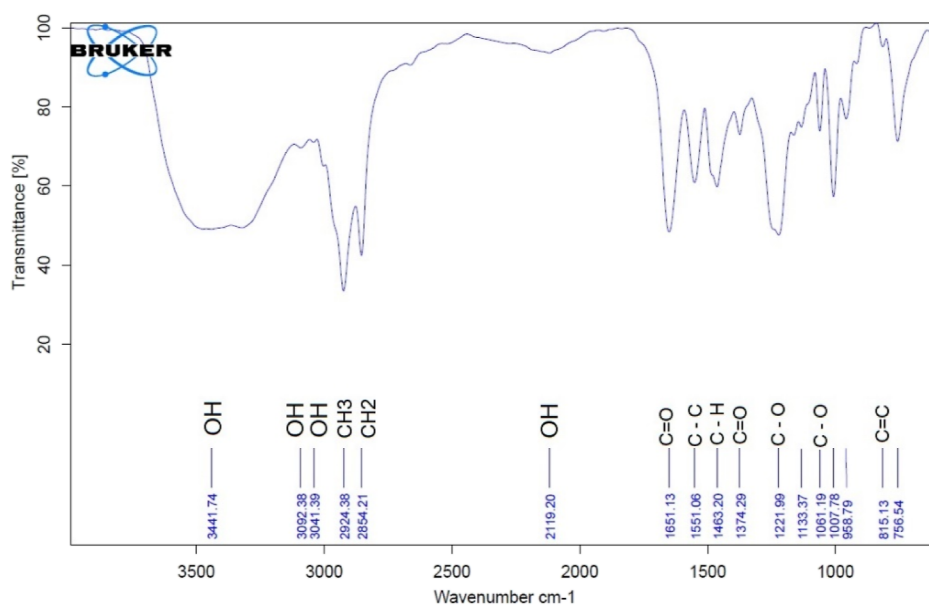


Figure 3. FTIR analysis of VES 2000 was used for preparation of the gel phase.

ature control can be achieved using a Peltier plate, a solvent plate with a hood, a Couette Peltier, or a CTD convection oven. This allows accurate temperatures from 40 to 1000 °C.

### 3. RESULTS AND DISCUSSION

**3.1. Characterization of Nanoparticles.** The characteristics and structure of the nanoparticles were investigated by using FESEM analysis. In order to check and identify the structure of the used nanoparticles, the FESEM analysis test with a field of view of 2.89 mm was conducted. Based on the obtained images, each nanoparticle has a unique structure with distinct characteristics. In Figure 2a, the structure of the iron oxide nanoparticle can be observed, which primarily consists of spherical or octagonal particles tightly packed together. The structural components of this nanoparticle are evenly distributed within the field of view, resulting in only a few empty spaces between them. This arrangement contributes to a more stable structure. In Figure 2b, the MgO nanoparticle exhibits a cluster-like structure with an interwoven and crusted state. Empty spaces of varying dimensions can be found both between these clusters and on their surface. The presence of cluster structures among the nanoparticles reduces their weight in larger volumes, which positively influences the formation of multiple connections and the creation of multiple bridges with micelles. In Figure 2c, the ZnO nanoparticle is depicted, characterized by a compact overall structure composed of 4- and 5-sided geometric shapes. One notable distinction is the presence of numerous empty spaces between these structures, along with a high dispersion in particle surface size and a lack of regular integration among them.

The Fourier transform infrared (FTIR) spectra of the VES2000 are shown in Figure 3. According to the results obtained from the FTIR test related to the used VES in this work, peaks at the wavenumber of 3441.74  $\text{cm}^{-1}$ , which indicate the presence of the OH functional group, are related to the hydroxyl compound. Additionally, the presence of sharper peaks indicates the presence of other functional groups that determine the overall structure of this substance. For example, at 2924.38  $\text{cm}^{-1}$ , methyl groups with  $\text{CH}_3$  bonds and at 2854.21  $\text{cm}^{-1}$ , methylene group with  $\text{CH}_2$  bonds were

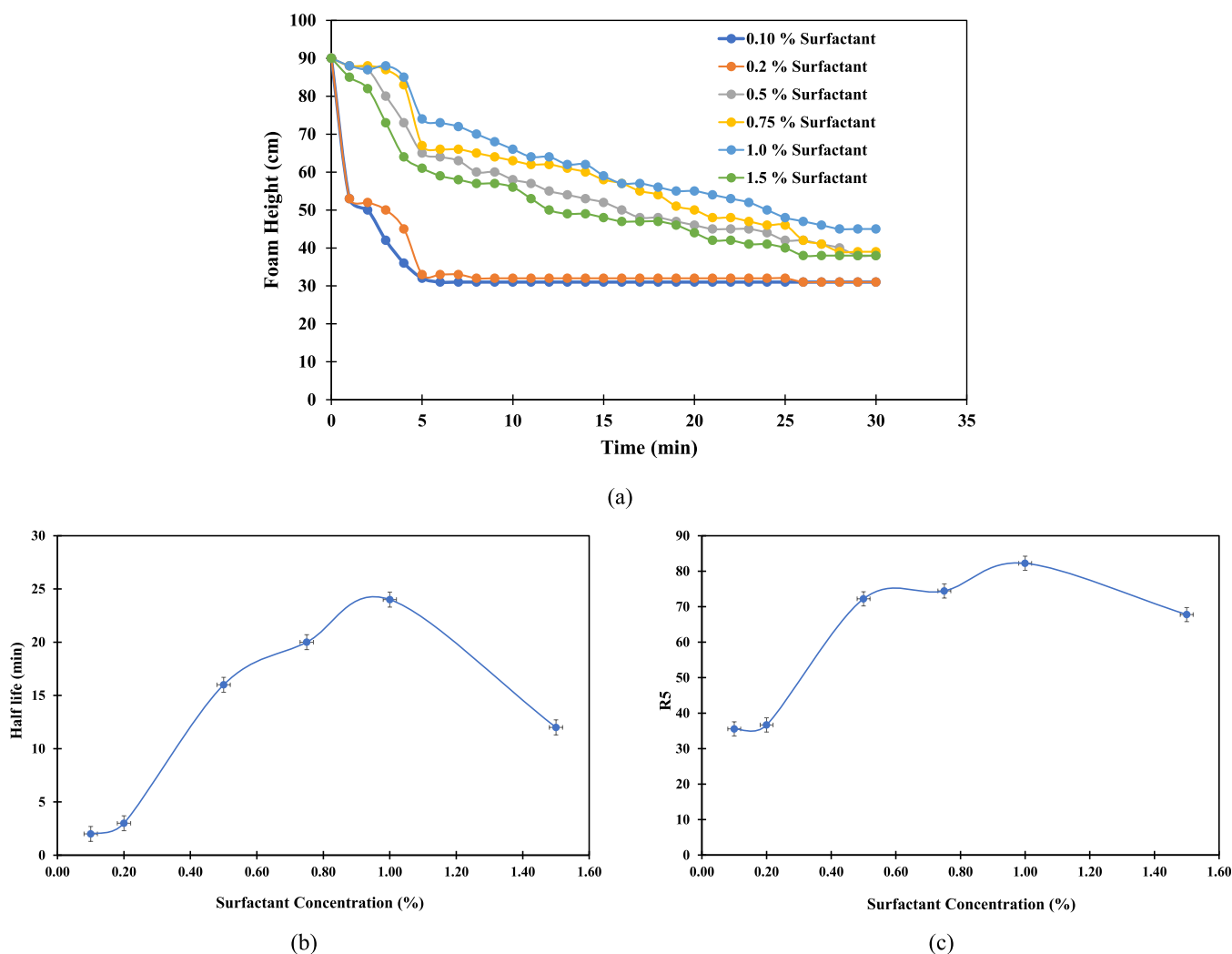
observed. Furthermore, the detected peak at the wavenumber of 1651.13  $\text{cm}^{-1}$  reveals the presence of carbonyl groups, which are assigned to carbon–oxygen bonds with double bonds. Furthermore, with the decrease in the wavenumber in the lower peaks, other groups and oxy compounds such as cyclic ether with single carbon–oxygen bonds, as well as the single bond of carbon with hydrogen, which are alkynes, are observed. The general properties of nanoparticles are given in Table 3 To obtain total pore volume, average diameter, and

Table 3. Textural and Surface Characteristics of the Synthesized Nanoparticles

nanoparticle	specific surface area, $A_{\text{BET}}$ ( $\text{m}^2\text{-g}^{-1}$ )	average pore diameter, $d_{\text{BET}}$ (nm)	average size, $d_{\text{aver}}$ (nm)	pore volume, $V_{\text{BJH}}$ ( $\text{cm}^3\text{-g}^{-1}$ )
$\text{Fe}_2\text{O}_3$	78.1	22.5	19.0	0.164
MgO	39.2	21.9	25.1	0.358
ZnO	30.8	19.1	29.9	0.201

surface area characteristics of the synthesized nanoparticles, nitrogen adsorption–desorption experiments were executed, and data were collected at the boiling point of  $\text{N}_2$  gas ( $-196$  °C). The BET and BJH (Barrett, Joyner, and Halenda) models were used to calculate the average diameters of the nanoparticles. The average diameters have been calculated from  $4V/S$  formula, where  $V$  and  $A$  are the pore volume and specific surface area of the nanoparticles, respectively.<sup>61</sup>

**3.2. Optimum Surfactant Concentration.** As explained, the stability of the foam is dependent on the texture and structure of the foam bubbles. To determine the highest level of stability at different concentrations,  $R_5$  and half-life tests were performed. According to the obtained results, the highest value corresponds to a concentration of 1% wt of surfactant (Figure 4). At this concentration, after nitrogen gas was injected into the foam solution and it reached its maximum height, it exhibited the best stability compared to the other concentrations. Additionally, at a concentration of 1 wt % surfactant, the rate of foam height reduction was much lower than the others. In this case, the tissue network of the bubbles was very small, which also caused the formation of lamellae



**Figure 4.** Experiments for measuring the rate of foam height reduction to determine the optimal surfactant concentration: (a) measurement of the rate of foam height reduction at different concentrations, (b) surfactant half-life analysis at different concentrations, and (c)  $R_\zeta$  test analysis for different surfactant concentrations.

with the appropriate thickness. The thickness of the lamella has facilitated the movement of gas between the bubbles and prevented the collapse of the foam structure. Therefore, this foam exhibits the highest level of stability. However, at concentrations higher than 1 wt %, the stability of the foam decreased due to the surfactant concentration reaching its CMC and also resulted in a faster decrease in foam height.

**3.3. Determination of the Optimal VES Concentration.** It is crucial to determine the optimal concentration of the VES to achieve the best rheological stability in terms of viscosity. For this purpose, viscosity change evaluation tests were conducted at two different VES concentrations, 6 and 7.5 wt%. The tests were carried out in two stages. First, the environmental temperature was kept constant while the shear rate was varied from 0.1 to 1000  $\text{s}^{-1}$ , and the corresponding changes in viscosity were recorded. In the second stage, the optimal shear rate (100  $\text{s}^{-1}$ ) was determined, and the effect of increasing the temperature was assessed. The fluid's temperature was increased to 85  $^\circ\text{C}$ , and the variations in viscosity were observed over time for VES fluids with different concentrations. Furthermore, the impact of removing SDS from the solution with the best viscosity was also investigated. As per the results obtained, the highest viscosity was observed

in the 7.5 wt % VES solution under constant temperature conditions (Figure 5). At a shear rate of 100  $\text{s}^{-1}$ , the viscosity reached 73.44 cP. This experiment was repeated after removing the SDS from the solution, resulting in a decrease in viscosity to 65.45 cP in the 7.5 wt% VES solution. The presence of SDS promotes the formation of dense, white

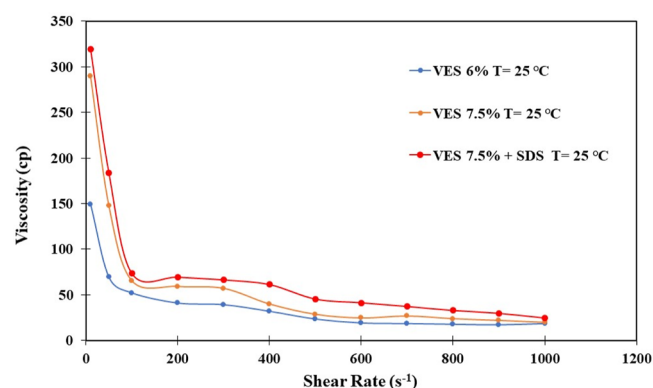


**Figure 5.** Changes in viscosity with an increasing shear rate at a constant temperature of 25  $^\circ\text{C}$  for different percentages of the VES.

micelles, thereby enhancing viscosity. Conversely, removing the SDS renders the micelles more fragile and prone to separation, reducing the gel-like state of the solution. Each test had a duration of 90 min.

In the solution containing 7.5 wt % VES and 1 wt % SDS, the rate of viscosity reduction at higher shear rates was lower than in the other solutions. Subsequently, at a temperature of 85 °C, the solution containing 7.5 wt % VES exhibited the best performance, with a viscosity of 185.214 cP at 80 °C (Figure 6). The highest viscosity observed in the 6 wt % VES solution

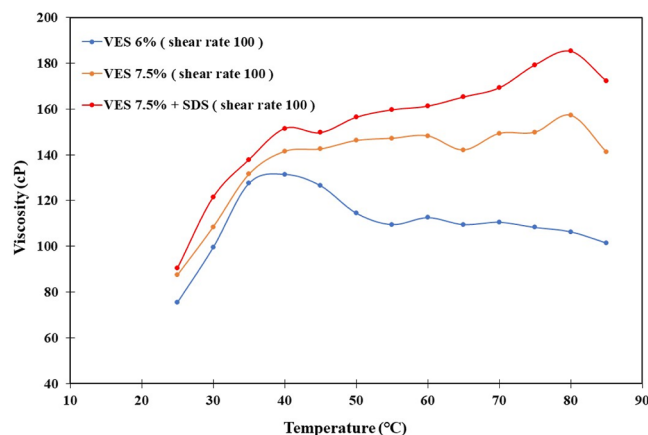


**Figure 6.** Change in the behavior of the VES at a constant shear rate with increasing temperature up to 85 °C for different percentages of the VES.

was at 40 °C, 131.45 cP. Increasing the VES concentration from 6 to 7.5 wt % also led to an increase in the solution's elasticity.

The viscosity of VES fluids exhibits remarkable sensitivity to temperature variations, especially when micelles are present. Micelles are self-assembled aggregates formed by surfactant molecules in a solution, wherein hydrophobic tails are buried inside the micellar core, while the hydrophilic heads are exposed to the solution. Micelles play a crucial role in enhancing fluid viscosity through entanglement and intermicellar interactions. At the macroscopic level, the temperature-induced viscosity increase in VES fluids with micelles primarily stems from changes in the solvent viscosity and

micellar elasticity. Higher temperatures reduce the solvent's viscosity, thereby decreasing its effect on the micelle's motion. However, the elasticity of the micelles increases due to reduced interactions and increased microstructural disorder, leading to a higher resistance to flow. In VES fluids, as the temperature increases, the viscosity typically increases to a certain critical temperature, known as the gelation temperature. This behavior is a result of increased micellar entanglement and enhanced intermolecular interactions within the micellar network. The gel network strengthens, leading to an overall increase in the viscosity of the VES fluid. However, beyond the gelation temperature, as the temperature decreases, the viscosity of the VES fluid starts to decrease. The reduction in viscosity is primarily attributed to the disruption of micellar structures caused by thermal energy. At lower temperatures, the reduced thermal energy allows the micelles to rearrange and relax, causing a decrease in the number of intermolecular interactions and resulting in a lower viscosity. This phenomenon can be attributed to the stronger intermolecular forces and highly entangled micellar networks within the VES fluids with a higher VES content. The increased VES concentration leads to a more interconnected network of micelles, forming a denser and stronger gel structure. As a result, the disruption of this network at lower temperatures becomes slower and requires more energy, resulting in a slower reduction of the viscosity over time.

**3.4. Effect of Metallic Nanoparticles on Improving the Rheological Performance of the Gel Solution.** In this stage of the experiment, three nanoparticles, Fe<sub>2</sub>O<sub>3</sub>, MgO, and ZnO, were synthesized and used at concentrations of 500, 1000, and 2000 ppm to study their effects on improvement of the rheological behavior of the viscoelastic solution. In the first part, at a constant ambient temperature, nine tests were performed in different concentrations of nanoparticles, with the shear rate varying from 0.1 to 1000 s<sup>-1</sup>. According to the obtained results given in Table 4, at a shear rate of 100 s<sup>-1</sup>, for Fe<sub>2</sub>O<sub>3</sub> nanoparticles, the highest viscosity value was observed at a concentration of 2000 ppm (182.91 cP). For ZnO and MgO, the highest viscosity was observed at 1000 ppm, which are 147.84 and 154.3 cP, respectively. The performances of MgO nanoparticles in improving viscosity at concentrations of 500 and 2000 ppm are almost similar, so considering that the concentration of 500 ppm of magnesium oxide is economical.

**Table 4.** Viscosity of VES Solution in the Presence of Metallic Nanoparticles at Variable Shear Rates

shear rate (s <sup>-1</sup> )	Fe <sub>2</sub> O <sub>3</sub>			ZnO			MgO		
	500 ppm	1000 ppm	2000 ppm	500 ppm	1000 ppm	2000 ppm	500 ppm	1000 ppm	2000 ppm
0.1	72449.3	37203.46	38182.51	19580.54	18601.48	12727.18	23496.74	21538.64	45035.87
1	11250.47	5674.77	5077.38	3086.06	4977.81	4778.68	5873.91	4579.55	3185.62
10	900.19	890.18	930.21	439.84	830.13	509.89	770.09	840.14	519.9
50	227.53	223.53	229.53	181.52	281.53	183.52	201.52	237.53	207.52
100	169.61	173.06	182.91	116.86	147.84	116.85	145.76	154.3	149.18
200	112.24	115.36	119.41	74.51	114.01	69.51	66.01	83.01	81.01
300	73.08	72.25	71.05	51.18	90.84	49.51	48.84	59.51	51.58
400	57.26	48.26	51.26	38.76	59.01	35.51	41.01	46.26	46.76
500	45.91	34.51	43.11	36.71	46.91	33.11	39.91	39.51	37.71
600	37.68	29.84	30.68	28.84	38.01	28.51	31.84	35.34	35.18
700	32.8	28.51	29.08	27.08	34.22	25.08	28.22	30.08	32.08
800	30.64	26.14	27.64	26.39	27.89	24.64	25.76	29.14	32.26
900	27.18	23.95	23.18	24.18	25.73	21.51	21.62	24.29	29.4
1000	25.21	22.71	22.11	21.31	24.11	19.61	23.01	23.21	24.41

Among all nanoparticles, the iron oxide nanoparticle has the best performance in improving fluid rheology. For instance, at 500 ppm, the viscosity of the fluid reached 169.61 cP at a shear rate of  $100 \text{ s}^{-1}$ , and the reduction in viscosity with the increasing shear rate is also lower than that with the other nanoparticles. This indicates an increased resistance of the fluid to flow (Table 4).

Micelles are self-assembling structures formed by surfactant molecules in a solution, and when iron oxide nanoparticles are introduced into a solution containing micelles, they can interact with the micelles through various microscopic mechanisms. One potential mechanism is the adsorption of iron oxide nanoparticles onto the surface of the micelles, where electrostatic forces, van der Waals forces, and steric hindrance play a role. These interactions can lead to the formation of a stable colloidal dispersion, where nanoparticles are embedded within or attached to the micellar structures. Another mechanism is the formation of aggregates or clusters of iron oxide nanoparticles within the micelles, modifying the micellar structure and leading to changes in rheological properties like viscosity. These nanoparticles act as physical cross-linking points that entangle and connect, forming a structured network that restricts fluid flow and results in increased resistance to deformation and thus higher viscosity. By examination of the microscopic properties of the micelles, it was observed that the presence of iron oxide nanoparticles increases the entanglement points within the micelles, creating a more interconnected structure. The higher cross-linking of the micelles improves the viscoelastic properties. Iron oxide nanoparticles have advantages over magnesium oxide as they can lead to a liquid gel state due to their special properties and interaction with the surrounding environment. All nanoparticles can potentially affect the rheological properties and state of the liquid gel, but their mechanisms are different. One of the key aspects investigated in this study was the impact of varying concentrations of different types of nanoparticles on the viscoelastic fluid viscosity behavior. The results shown in Figure 7 indicate that increasing the nanoparticle concen-

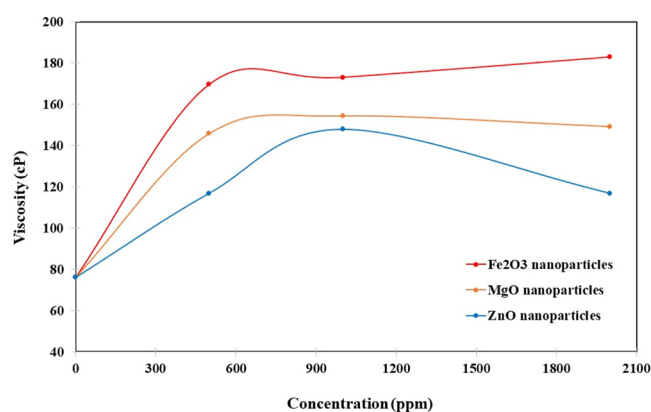


**Figure 7.** Effect of nanoparticle concentration on viscosity of VES solution.

tration up to 500 ppm leads to an increase in fluid viscosity. At a concentration of 1000 ppm, the viscosity increase was less pronounced, but the fluid remained stable. However, when the concentration was increased to 2000 ppm, a decrease in fluid viscosity was observed, with this reduction being less significant for iron oxide nanoparticles. The most optimal

performance of the nanoparticles was observed at a concentration of 500 ppm, aligning with the findings of a study reported by Raj KA et al.<sup>62</sup> In their research, it was demonstrated that while higher nanoparticle concentrations lead to increased fluid viscosity, no further significant changes were noted beyond the 750 ppm concentration level.<sup>62</sup> At elevated concentrations, the significance of surface area and charge diminishes as the connections between the nanoparticles become more prevalent, potentially leading to aggregation of excessive nanoparticles due to their heightened surface energy, thereby impeding viscosity.

The existence of metallic nanoparticles can improve the rheological behavior of fluids in contact with the oil. This performance improvement can facilitate emulsification and improve the flow resistance. Among the viscoelastic fluids, nanoparticles that improve viscosity by increasing the network structure of micelles, when in contact with oil, can aid the emulsification process and promote a better dispersion of oil among the micelles. This dispersion is achieved through strong surface interactions between nanoparticles and oil droplets, ultimately leading to the encapsulation of oil in the fluid matrix. Additionally, the presence of nanoparticles can increase the flow resistance when in contact with oil. The metallic nanoparticles create a stronger network and more connection points between the micelles, resulting in an increased viscosity and resistance to deformation of the fluid. Compared to other studied nanoparticles in this work, the iron oxide nanoparticle can form more connection points or entanglements with surfactant molecules, causing the solution to have higher resistance to breakage and changes in state as the shear rate increases. This is why, during the experiment, the iron oxide nanoparticle showed a lower rate of viscosity reduction than the other nanoparticles. Another important factor for improving fluid rheology with iron oxide is its ability to exhibit special lubrication due to its surface characteristics. As the shear rate increases, this nanoparticle can form a lubricating layer or boundary lubrication film, reducing friction between adjacent layers and helping maintain viscosity and reduce the rate of viscosity reduction at higher shear rates. In the second part, at a constant shear rate of  $100 \text{ s}^{-1}$ , the temperature was increased from 25 to 85 °C, and the effect of temperature increase on the improvement of fluid performance in the presence of different nanoparticles was evaluated. The obtained results are shown in Figure 8a–c. According to the results obtained, the Fe<sub>2</sub>O<sub>3</sub> nanoparticle demonstrated better performance at higher temperatures. It was able to maintain an increasing trend in solution viscosity up to 80 °C, after which the viscosity started to decrease. This resulted in the fluid reaching a viscosity of 386.14 cP, which is the highest value compared to those of the other nanoparticles. However, increasing the concentration of the iron oxide nanoparticles caused a decrease in thermal resistance. These interactions are vital in maintaining the structural integrity and viscosity of the fluid at high temperatures, where molecular movement and thermal energy increase. The use of nanoparticles as physical binders can stabilize the structural network of surfactants and prevent their decomposition under thermal stress. In Figure 9, different studied nanoparticles at an optimum concentration of 500 ppm are given. It is demonstrated that the Fe<sub>2</sub>O<sub>3</sub> nanoparticle at a concentration of 500 ppm resulted in the highest performance for enhancement of VES rheology.

Additionally, analysis of the FESEM images in Figure 10, which reveal the overall structure between the nanoparticles



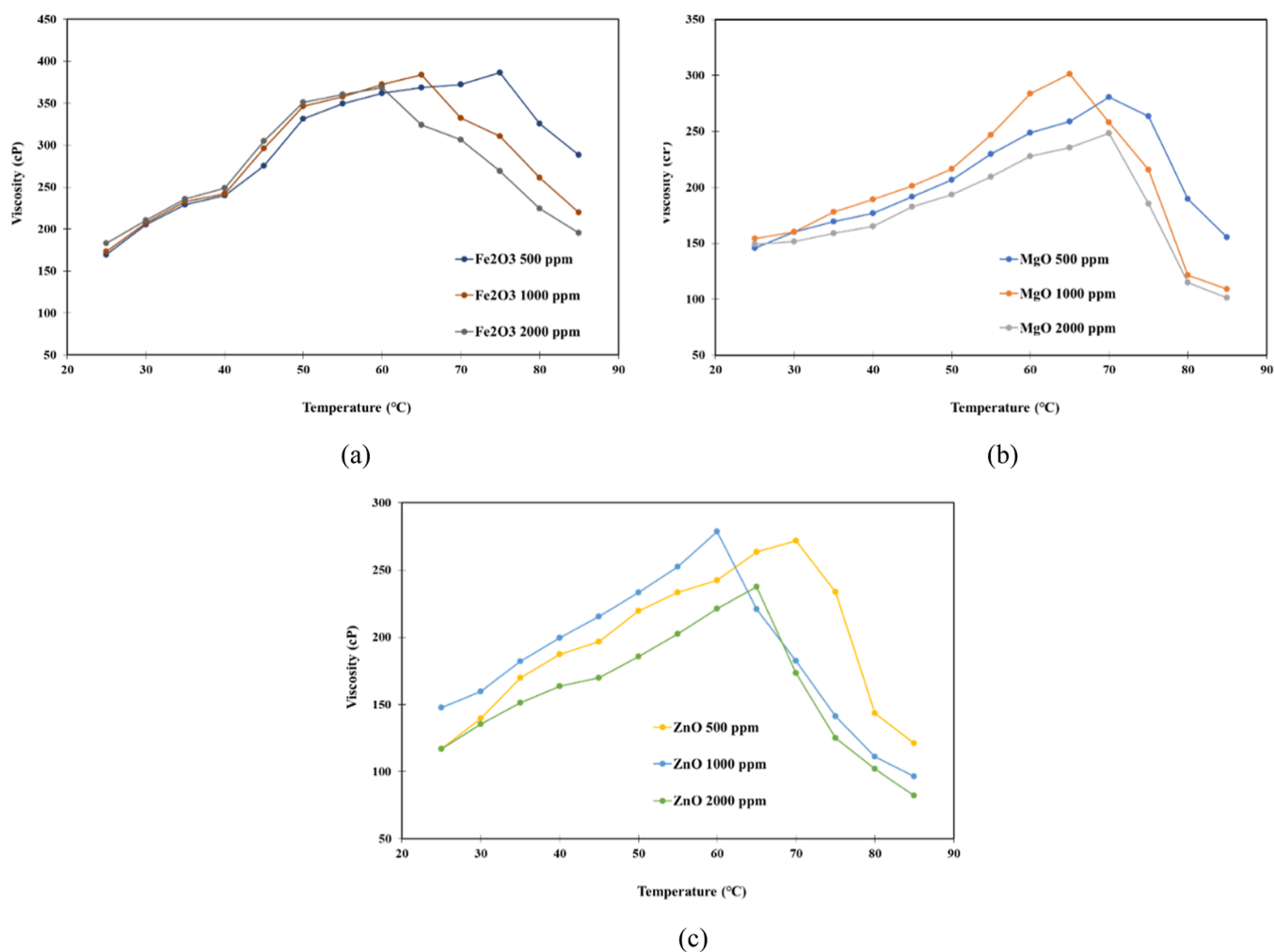


**Figure 8.** Change in the viscosity of VES solution with increasing temperature in the presence of different concentrations of metallic nanoparticles: (a) Fe<sub>2</sub>O<sub>3</sub> nanoparticle, (b) MgO nanoparticle, and (c) ZnO nanoparticle.

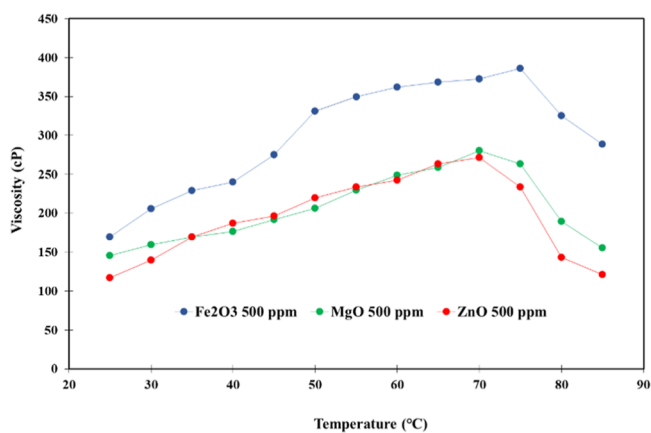


**Figure 9.** Viscosity of VES solution versus temperature for the optimum concentration of studied nanoparticles.

and micelles, demonstrates that in a solution containing iron oxide nanoparticles and VES solution, the significantly smaller size of these particles and their high abundance in the solution result in numerous physical connections between micelles (Figure 10a). This leads to the formation of a saturated structure with minimal empty space and a high thickness. The presence of these physical connections among micelles

enhances resistance to fluid flow and temperature increase. With increasing temperature, the strength between micelles provided by the iron oxide nanoparticles prevents the structure of the micelles from being destroyed or broken by the increase in the kinetic energy. In the case of VES solution with magnesium oxide nanoparticles (Figure 10b), observations indicate that cluster structures between micelles are preserved. These structures facilitate the formation of physical connections between micelles of extended length. Due to the high distribution of cluster structures, multiple connections are established between micelles, compacting the overall structure and resulting in empty spaces between them. Furthermore, the cluster structures can connect micelles in various ways, and as mentioned before, they have less weight in larger volumes. These factors contribute to superior performance compared to that of iron oxide nanoparticles. Furthermore, analysis of FESEM images of a VES solution with zinc oxide nanoparticles (Figure 10c) reveals that the connection between the micelles is layered. Each layer possesses different surface areas with varying compressive strengths compared to other nanoparticles. The general field of view of this solution displays numerous empty spaces, which diminishes the stability of the connections between micelles.

**3.5. Effect of Nanoparticles on Improving the Carrying Capacity of Bentonite Particles.** As seen, the

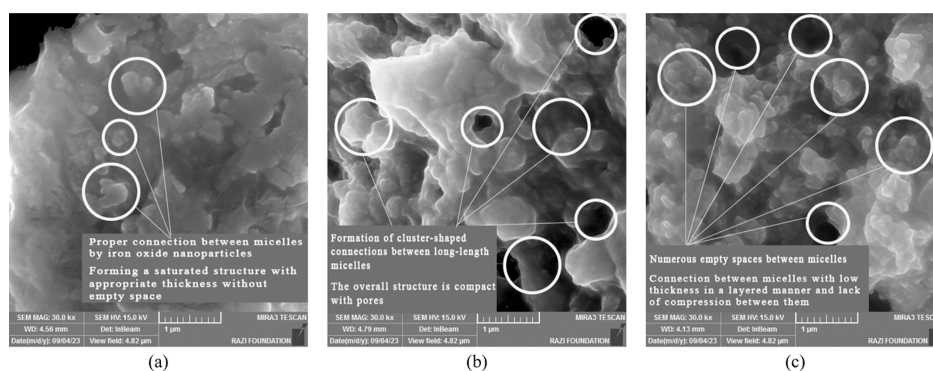


**Figure 10.** FESEM images of VES solution in the presence of different nanoparticles: (a) treatment of VES solution with  $\text{Fe}_2\text{O}_3$ , (b) treatment of VES solution with  $\text{MgO}$ , and (c) treatment of VES solution with  $\text{ZnO}$ .

**Table 5. Residence Time of Bentonite on the Surface of the Solution and the Settling Time of Bentonite in the Solution in the Presence of Different Nanoparticles at Varying Temperatures**

#	solution	time for carry bentonite, $T = 25\text{ }^\circ\text{C}$	time for carry bentonite, $T = 85\text{ }^\circ\text{C}$	settling time, $T = 25\text{ }^\circ\text{C}$	settling time, $T = 85\text{ }^\circ\text{C}$
1	VES (7.5%) + SDS + distilled water + $\text{CaCl}_2$	2 h, 25 min	4 h, 32 min	2 h	6 h, 33 min
2	VES (7.5%) + SDS + distilled water + $\text{CaCl}_2$ + $\text{MgO}$ (500 ppm)	3 h	6 h	2 h, 42 min	7 h, 36 min
3	VES (7.5%) + SDS + distilled water + $\text{CaCl}_2$ + $\text{MgO}$ (1000 ppm)	3 h, 15 min	5 h, 11 min	2 h, 11 min	8 h, 10 min
4	VES (7.5%) + SDS + distilled water + $\text{CaCl}_2$ + $\text{MgO}$ (2000 ppm)	2 h, 43 min	6 h, 28 min	1 h, 50 min	7 h
5	VES (7.5%) + SDS + distilled water + $\text{CaCl}_2$ + $\text{ZnO}$ (500 ppm)	3 h	6 h	1 h, 31 min	6 h, 8 min
6	VES (7.5%) + SDS + distilled water + $\text{CaCl}_2$ + $\text{ZnO}$ (1000 ppm)	3 h, 13 min	6 h, 31 min	2 h, 35 min	7 h, 15 min
7	VES (7.5%) + SDS + distilled water + $\text{CaCl}_2$ + $\text{ZnO}$ (2000 ppm)	2 h, 50 min	5 h	1 h, 37 min	6 h
8	VES (7.5%) + SDS + distilled water + $\text{CaCl}_2$ + $\text{Fe}_2\text{O}_3$ (500 ppm)	4 h, 35 min	7 h	2 h, 39 min	8 h, 44 min
9	VES (7.5%) + SDS + distilled water + $\text{CaCl}_2$ + $\text{Fe}_2\text{O}_3$ (1000 ppm)	3 h, 50 min	6 h, 12 min	2 h, 14 min	7 h, 5 min
10	VES (7.5%) + SDS + distilled water + $\text{CaCl}_2$ + $\text{Fe}_2\text{O}_3$ (2000 ppm)	4 h, 50 min	7 h	3 h, 48 min	7 h, 38 min

addition of nanoparticles was able to improve the elastic properties of the solution. At this stage of the test, the ability to carry bentonite particles by the solution and the properties of the particle suspension were investigated in two different parts. In the first part, the time it takes for bentonite to remain on the surface of the fluid without absorbing liquid was evaluated in states without nanoparticles and with the nanoparticles. In the second part, the effect of adding nanoparticles to the solution on the sedimentation rate of the bentonite particles was investigated.

According to the obtained results, in general, the addition of the nanoparticles has improved both the ability to carry particles and the function of keeping particles suspended in solution (Table 5). However, the effect of each nanoparticle is different. In general, the two nanoparticles of magnesium oxide and iron oxide have shown better performance. In a fluid without the nanoparticles, the duration of carrying bentonite on the surface of the fluid was measured to be about 2 h and 25 min, and after that, the time it took for bentonite particles to settle was also measured for 2 h at ambient temperature. Next, by adding nanoparticles at different concentrations, the retention time of these particles in the gel solution increased. Regarding the concentration of 500 ppm of magnesium oxide and iron oxide, the duration of carrying bentonite on the solution surface at ambient temperature increased to 3 h and 4 h and 35 min, respectively. In this section, the performances of magnesium oxide and zinc oxide nanoparticles were similar to each other, but in the particle sedimentation test, zinc oxide nanoparticles showed weaker performance.

In the second part, the settling times of bentonite particles in the two nanoparticles of magnesium oxide and iron oxide were

measured as 2 h and 42 min and 2 h and 39 min, respectively, at ambient temperature. Next, to assess the rheological behavior of the solution in terms of particle suspension, the temperature was increased to  $85\text{ }^\circ\text{C}$ , and the same tests were resumed. According to the results in Table 5, increasing the temperature in the presence of nanoparticles has improved the fluid's rheological properties and viscosity. This improvement also positively affects the performance of particle transport. In the fluid sample without the nanoparticles, the transport time for bentonite increases to 4 h and 32 min. The addition of nanoparticles at various concentrations further enhances this effect. In the case of 500 ppm concentrations of  $\text{MgO}$  and  $\text{Fe}_2\text{O}_3$  nanoparticles, the duration of bentonite transport on the fluid's surface increases to 6 and 7 h, respectively. In the second part of the test,  $\text{MgO}$  and  $\text{Fe}_2\text{O}_3$  nanoparticles exhibited superior performance. They demonstrated the lowest sedimentation rate at high temperatures, with iron oxide nanoparticles showing a sedimentation period of approximately 8 h and 44 min. To comprehensively examine the effect of  $\text{Fe}_2\text{O}_3$  nanoparticles on improving the fluid's ability to transport particles, physical and chemical parameters on a microscopic scale must be considered. As observed in the previous steps, compared with other nanoparticles,  $\text{Fe}_2\text{O}_3$  nanoparticles led to the higher viscosity of the fluid under identical conditions. Generally, by increasing viscosity and improving rheological behavior, iron oxide nanoparticles form a coherent network that bridges particles and enhances mutual attraction between them. Consequently, this network counteracts the downward force of gravity. Additionally, the modified surface charge of iron oxide nanoparticles results in increased electrostatic repulsion and the creation of a spatial barrier

**Table 6. Stability of the Gelation State of VES Solution in the Presence of Nanoparticles and at Different Temperatures**

solution		time for gel breaking, $T = 25\text{ }^{\circ}\text{C}$	time for gel breaking, $T = 85\text{ }^{\circ}\text{C}$
1	VES (7.5%) + SDS + distilled water + $\text{CaCl}_2$	5 h, 20 min	11 h
2	VES (7.5%) + SDS + distilled water + $\text{CaCl}_2$ + MgO (500 ppm)	7 h	15 h, 35 min
3	VES (7.5%) + SDS + distilled water + $\text{CaCl}_2$ + MgO (1000 ppm)	7 h, 45 min	16 h, 48 min
4	VES (7.5%) + SDS + distilled water + $\text{CaCl}_2$ + MgO (2000 ppm)	6 h	16 h
5	VES (7.5%) + SDS + distilled water + $\text{CaCl}_2$ + ZnO (500 ppm)	5 h, 35 min	13 h
6	VES (7.5%) + SDS + distilled water + $\text{CaCl}_2$ + ZnO (1000 ppm)	7 h, 38 min	15 h, 20 min
7	VES (7.5%) + SDS + distilled water + $\text{CaCl}_2$ + ZnO (2000 ppm)	5 h, 50 min	13 h, 40 min
8	VES (7.5%) + SDS + distilled water + $\text{CaCl}_2$ + $\text{Fe}_2\text{O}_3$ (500 ppm)	7 h, 50 min	17 h, 45 min
9	VES (7.5%) + SDS + distilled water + $\text{CaCl}_2$ + $\text{Fe}_2\text{O}_3$ (1000 ppm)	6 h, 25 min	15 h, 50 min
10	VES (7.5%) + SDS + distilled water + $\text{CaCl}_2$ + $\text{Fe}_2\text{O}_3$ (2000 ppm)	7 h, 15 min	16 h, 25 min

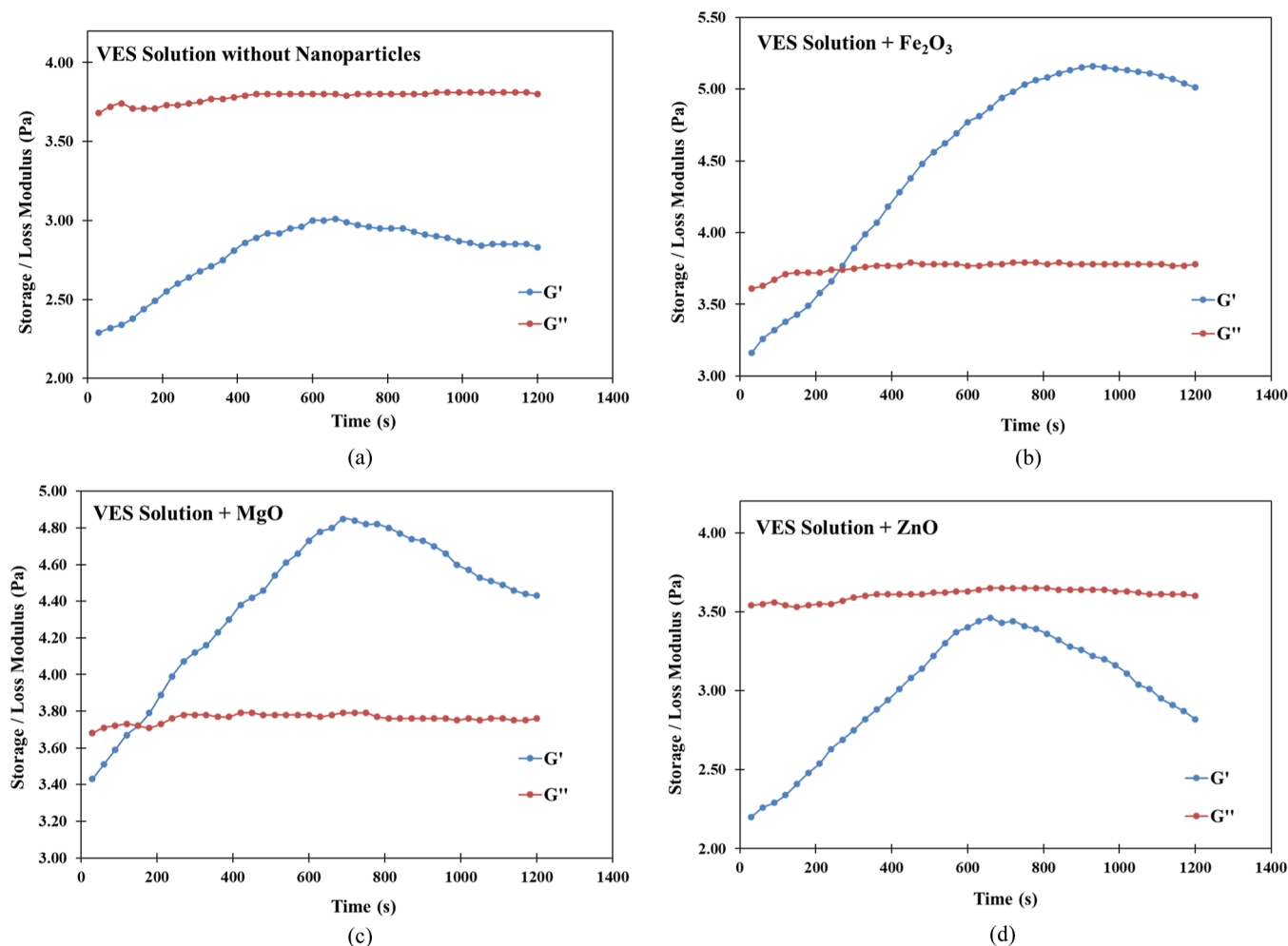


**Figure 11.** Changes of storage modulus ( $G'$ ) and loss modulus ( $G''$ ) of VES solution in the absence and presence of different nanoparticles: (a) VES solution without nanoparticles, (b) VES solution with  $\text{Fe}_2\text{O}_3$  nanoparticle at 500 ppm, (c) VES solution with MgO nanoparticle at 500 ppm, and (d) VES solution with ZnO nanoparticle at 500 ppm.

within the fluid. This improves the colloidal stability and prevents particle sedimentation. The presence of the nanoparticles deeply influences the dynamics of suspension and colloids in the gel fluid. According to the Stokes' law, sedimentation behavior is influenced by the fluid's density and viscosity, with higher viscosity leading to a lower sedimentation rate for particles. In general, the microscopic interactions obtained through the adsorption of nanoparticles onto bentonite platelets increase the effective mass of the particles. Consequently, in a viscous fluid, the sedimentation rate of the particles decreases. These interactions also impact

the critical flocculation concentration of the suspension and shift the equilibrium toward a more stable colloidal system due to the steric stabilization provided by the nanoparticles. The affinity between iron oxide and bentonite particles creates a spatial barrier that acts as an energy barrier preventing the accumulation and settlement of particles.

**3.6. Investigating the Preservation of the Gelation State in the Presence of Nanoparticles.** In this step, all of the solutions were placed in a static state, and the duration of maintaining their gel state was measured. In the solution without the nanoparticles, the state of fluid gelation was

maintained at ambient temperature for about 5 h and 20 min and at 85° for about 11 h (Table 6). This effect was improved by adding different nanoparticles to gels, so that with the addition of iron oxide nanoparticles at a concentration of 500 ppm at ambient temperature, the state of gelation of the fluid increased up to 7 h and 50 min, and at high temperature, this period of time reached about 17 h and 45 min. The effectiveness of fluid gelation was evaluated by observation so that after a few hours, the complete fluid changed from the gel state to a completely liquid state. According to the obtained results, the best performance was related to iron oxide nanoparticles. The presence of these nanoparticles in the fluid acts as a physical connection between adjacent micelles. Surfactant molecules gather in micelles in a way that is sensitive to the presence of nanoparticles. The surfaces of nanoparticles can absorb surfactant molecules, which leads to a change in shape or better reconstruction of micelles. As seen in the previous tests, increasing the temperature generally increases the viscosity of the solution, but after a certain temperature, the state of gelation of the fluid is broken, and the viscosity of the fluid decreases rapidly (Table 6). The presence of nanoparticles in these solutions increases their stability and temperature capacity. VES liquids can lose their structure at high temperatures because the kinetic energy entered overcomes the forces of maintaining the network of micelles, but by adding thermally stable nanoparticles in the connection between the micelles, they can maintain their integrity and continue to provide structural support to the micelles and maintain the gel structure even at high temperatures.

**3.7. Effect of Nanoparticles on Changes in Storage Modulus ( $G'$ ) and Loss Modulus ( $G''$ ).** In the study of rheology, storage modulus ( $G'$ ) and loss modulus ( $G''$ ) are important parameters used to describe the viscoelastic behavior of materials. Generally, the storage modulus represents the elastic response of a material in its ability to store energy upon exposure to stress or deformation. This parameter quantitatively shows the ability of the material to return to its original shape after the stress is removed. On the other hand, the loss modulus represents the material's ability to dissipate energy when exposed to stress. When the  $G'$  parameter is greater than  $G''$  or  $G'$  is dominant in some way, the material exhibits more elastic behavior than viscous behavior. This means that the material can resist deformation and effectively recover its original shape, showing solid-like behavior. During this experiment, the  $G'$  and  $G''$  parameters were measured for 20 min, considering fixed parameters such as a gamma amplitude of 50% and an angular frequency of 100 rad/s.

The results of changes in parameters  $G'$  and  $G''$  without and with nanoparticles at a concentration of 500 ppm are shown in Figure 11. In the VES solution without the nanoparticles, the  $G''$  parameter was generally dominant, indicating viscous behavior, and as is shown, in the considered time frame, the  $G'$  parameter could not exceed  $G''$  (Figure 11a). However, by adding nanoparticles, the  $G'$  value became closer to  $G''$ . By the addition of  $\text{Fe}_2\text{O}_3$  and  $\text{MgO}$  nanoparticles, the  $G'$  parameter became dominant and easily surpassed the  $G''$ , indicating elastic behavior with more stored energy than other nanoparticles (Figure 11b,c). On the other hand, the energy storage,  $G'$ , increased by approximately 5 Pa. For the  $\text{ZnO}$  nanoparticle, it almost reached 3.5 Pa, but it still could not surpass the  $G''$ , indicating a viscous state with high elasticity. During this stage of the test, iron oxide nanoparticles at a

concentration of 500 ppm exhibited the best performance in examining the fluid's elastic behavior.

#### 4. CONCLUSIONS

Metallic-based nanoparticles can act as stabilizers and dispersants for solid particles suspended in the fluid medium. They inhibit particle agglomeration and settling, thereby preventing blockages in the fractures and improving the overall efficiency of the fracturing process. Furthermore, the addition of metallic nanoparticles can modify the fluid's thermal behavior, allowing it to withstand high-temperature conditions encountered in deep reservoirs. This thermal stability ensures that the fracturing fluid maintains its performance and does not degrade or lose its desired properties, even in challenging environments. In this study, the effects of adding main metallic nanostructures,  $\text{Fe}_2\text{O}_3$ ,  $\text{MgO}$ , and  $\text{ZnO}$  nanoparticles, on improving the performance of viscoelastic fluids were investigated. Moreover, through the microscopic study, the effects of nanostructures on micelles shape and behavior were assessed. In general, the main results obtained in this work are as follows:

- The optimal concentration for achieving the best viscosity stability in VES solutions was found to be 7.5 wt %. The presence of SDS enhanced viscosity by promoting the formation of dense and white micelles. Temperature variations had a significant impact on viscosity, with higher temperatures increasing micellar elasticity and resistance to flow. Beyond the gelation temperature, decreasing temperatures led to a decrease in viscosity due to the disruption of micellar structures caused by thermal energy.
- Iron oxide nanoparticles demonstrated superior performance in improving fluid rheology by minimizing viscosity reduction and enhancing the flow resistance compared to that of other tested nanoparticles. This improvement is attributed to their high specific surface area and the increased entanglement points within the micelles, resulting in a more interconnected structure with improved viscoelastic properties.
- Analysis of FESEM images revealed that iron oxide nanoparticles formed numerous physical connections between the micelles in VES solution, creating a saturated structure with high thickness and minimal empty space. These connections enhanced resistance to fluid flow and temperature increase. Magnesium oxide nanoparticles preserved cluster structures and compacted the overall structure, and zinc oxide nanoparticles formed layered connections that resulted in empty spaces and reduced connection stability. Overall, the iron oxide nanoparticles demonstrated the strongest physical connections and stability in the VES solution.
- The addition of magnesium oxide and iron oxide nanoparticles improved the suspension and carrying capacity of a solution for bentonite particles. The retention time of bentonite on the fluid's surface was increased, with magnesium oxide and iron oxide demonstrating the best performance. Nanoparticles reduced the sedimentation rate of bentonite particles, with magnesium oxide and iron oxide showing the lowest settling times. Increasing the temperature further enhanced the rheological properties and viscosity of the solution, aiding in particle transport.

- Iron oxide nanoparticles were found to greatly enhance the gelation of the fluid by acting as physical connections between the micelles, improving stability and structure. The absorption of surfactant molecules by the nanoparticles further contributed to micelle reconstruction and shape change. The presence of iron oxide nanoparticles allowed the gel structure to be maintained even at high temperatures, preventing a rapid decrease in viscosity. Generally, iron oxide nanoparticles displayed the best performance in enhancing fluid gelation and stability.
- The solution without nanoparticles displayed largely viscous behavior, but the addition of the magnesium oxide and iron oxide nanoparticles improved its elastic behavior. Iron oxide nanoparticles at a concentration of 500 ppm had the greatest impact on enhancing the solution's elastic behavior, with a notable increase in energy storage. These results demonstrate the potential of nanoparticles, particularly iron oxide, in modifying the viscoelastic properties of materials.
- The pH of the fluid medium can strongly affect the performance of the nanoparticle–VES solutions. It is strongly suggested for future research studies as it is an ongoing subject for the authors in some industrial projects.

## ■ ASSOCIATED CONTENT

### Data Availability Statement

The data underlying this study are available in the published article and its [Supporting Information](#).

### SI Supporting Information

The Supporting Information is available free of charge at <https://pubs.acs.org/doi/10.1021/acsomega.4c03000>.

Chemical samples information ([PDF](#))

## ■ AUTHOR INFORMATION

### Corresponding Author

Saber Mohammadi – *Petroleum Engineering Department, Research Institute of Petroleum Industry (RIPI), Tehran 14665-1998, Iran*; [orcid.org/0000-0002-2919-6719](https://orcid.org/0000-0002-2919-6719);  
Email: [mohammadi.sab@gmail.com](mailto:mohammadi.sab@gmail.com)

### Authors

Alimohammad Hemmat – *Department of Chemical Engineering, Isfahan University of Technology, Isfahan 84156-83111, Iran*

Hamidreza Afifi – *Petroleum Engineering Department, Research Institute of Petroleum Industry (RIPI), Tehran 14665-1998, Iran*

Fatemeh Mahmoudi Alemi – *Petroleum Engineering Department, Research Institute of Petroleum Industry (RIPI), Tehran 14665-1998, Iran*

Complete contact information is available at:  
<https://pubs.acs.org/10.1021/acsomega.4c03000>

### Notes

The authors declare no competing financial interest.

## ■ ACKNOWLEDGMENTS

The authors acknowledge the *Research Institute of Petroleum Industry (RIPI)* for providing funding under the grant of industrial project (no. 44481352) and experimental facilities.

Also, the *Energy Chemical Co. Semnan* is greatly appreciated for supplying the materials.

## ■ REFERENCES

- (1) Barati, R.; Liang, J. T. A review of fracturing fluid systems used for hydraulic fracturing of oil and gas wells. *J. Appl. Polym. Sci.* **2014**, *131* (16), 40735..
- (2) Baruah, A.; Shekhawat, D. S.; Pathak, A. K.; Ojha, K. Experimental investigation of rheological properties in zwitterionic-anionic mixed-surfactant based fracturing fluids. *J. Pet. Sci. Eng.* **2016**, *146*, 340–349.
- (3) Kefi, S.; Lee, J.; Pope, T.; Sullivan, P.; Nelson, E.; Hernandez, A. Expanding applications for viscoelastic surfactants. *Oilfield Rev.* **2004**, *16* (4), 10–23.
- (4) You, Q.; Wang, H.; Zhang, Y.; Liu, Y.; Fang, J.; Dai, C. Experimental study on spontaneous imbibition of recycled fracturing flow-back fluid to enhance oil recovery in low permeability sandstone reservoirs. *J. Pet. Sci. Eng.* **2018**, *166*, 375–380.
- (5) Holmberg, K.; Jönsson, B.; Kronberg, B.; Lindman, B. *Surfactants Polymers in Aqueous Solution*; Wiley-Blackwell, 2002.
- (6) Emrani, A. S.; Nasr-El-Din, H. A. An experimental study of nanoparticle-polymer-stabilized CO<sub>2</sub> foam. *Colloids Surf., A* **2017**, *524*, 17–27.
- (7) Fischer, P.; Rehage, H.; Grüning, B. Rheologische Eigenschaften von Dimersäurebetainlösungen/Rheological properties of dimer acid betaine solutions. *Tenside, Surfactants, Deterg.* **1994**, *31* (2), 99–108.
- (8) Róžańska, S. Rheology of wormlike micelles in mixed solutions of cocoamidopropyl betaine and sodium dodecylbenzenesulfonate. *Colloids Surf., A* **2015**, *482*, 394–402.
- (9) Wu, X.; Zhang, Y.; Sun, X.; Huang, Y.; Dai, C.; Zhao, M. A novel CO<sub>2</sub> and pressure responsive viscoelastic surfactant fluid for fracturing. *Fuel* **2018**, *229*, 79–87.
- (10) Silva, K. N.; Novoa-Carballal, R.; Drechsler, M.; Müller, A. H.; Penott-Chang, E. K.; Müller, A. J. The influence of concentration and pH on the structure and rheology of cationic surfactant/hydrotrope structured fluids. *Colloids Surf., A* **2016**, *489*, 311–321.
- (11) Qiu, L.; Shen, Y.; Wang, C. pH-and KCl-induced formation of worm-like micelle viscoelastic fluids based on a simple tertiary amine surfactant. *J. Pet. Sci. Eng.* **2018**, *162*, 158–165.
- (12) Mao, J.; Tian, J.; Zhang, W.; Yang, X.; Zhang, H.; Lin, C.; Zhang, Y.; Zhang, Z.; Zhao, J. Effects of a counter-ion salt (potassium chloride) on gemini cationic surfactants with different spacer lengths. *Colloids Surf., A* **2019**, *578*, 123619.
- (13) Kwiatkowski, A. L.; Molchanov, V. S.; Orekhov, A. S.; Vasiliev, A. L.; Philippova, O. E. Impact of salt co-and counterions on rheological properties and structure of wormlike micellar solutions. *J. Phys. Chem. B* **2016**, *120* (49), 12547–12556.
- (14) Rojas, M. R.; Müller, A. J.; Sáez, A. E. Shear rheology and porous media flow of wormlike micelle solutions formed by mixtures of surfactants of opposite charge. *J. Colloid Interface Sci.* **2008**, *326* (1), 221–226.
- (15) Van Zanten, R. Stabilizing viscoelastic surfactants in high-density brines. *SPE Drill. Completion* **2011**, *26* (04), 499–505.
- (16) Manet, S.; Karpichev, Y.; Bassani, D.; Kiagus-Ahmad, R.; Oda, R. Counteranion effect on micellization of cationic gemini surfactants 14–2-14: Hofmeister and other counterions. *Langmuir* **2010**, *26* (13), 10645–10656.
- (17) Ahmadi, M. A.; Sheng, J. Performance improvement of ionic surfactant flooding in carbonate rock samples by use of nanoparticles. *Pet. Sci.* **2016**, *13*, 725–736.
- (18) Shahmarvand, S.; Ameli, F.; Mohammadi, S.; Hossein Abad Fouladi, K. Experimental investigation on the stability of foam using combination of anionic and zwitterionic surfactants: A screening scenario to obtain optimum compound. *J. Dispersion Sci. Technol.* **2023**, 1–12.
- (19) Huang, T.; Crews, J. B. Solids suspension with nanoparticle-associated viscoelastic surfactant micellar fluids. U.S. Patent 9,556,376 B2, 2017.

- (20) Lv, Q.; Li, Z.; Li, B.; Li, S.; Sun, Q. Study of nanoparticle-surfactant-stabilized foam as a fracturing fluid. *Ind. Eng. Chem. Res.* **2015**, *54* (38), 9468–9477.
- (21) Huang, T.; Crews, J. B.; Willingham, J. R. Nanoparticles for formation fines fixation and improving performance of surfactant structure fluids. In *IPTC: International Petroleum Technology Conference*; EAGE, 2008.
- (22) Zhang, Y.; Dai, C.; Qian, Y.; Fan, X.; Jiang, J.; Wu, Y.; Wu, X.; Huang, Y.; Zhao, M. Rheological properties and formation dynamic filtration damage evaluation of a novel nanoparticle-enhanced VES fracturing system constructed with wormlike micelles. *Colloids Surf., A* **2018**, *553*, 244–252.
- (23) Chauhan, G.; Ojha, K.; Baruah, A. Effects of nanoparticles and surfactant charge groups on the properties of VES gel. *Braz. J. Chem. Eng.* **2017**, *34*, 241–251.
- (24) Ihejirika, B.; Dosunmu, A.; Eme, C. Performance evaluation of guar gum as a carrier fluid for hydraulic fracturing. In *SPE Nigeria annual international conference and exhibition*, 2015.
- (25) Yang, J.; Guan, B.; Lu, Y.; Cui, W.; Qiu, X.; Yang, Z.; Qin, W. Viscoelastic evaluation of gemini surfactant gel for hydraulic fracturing. In *SPE European Formation Damage Conference and Exhibition*, 2013.
- (26) Zhang, D.; Lu, X.; Li, Y.; Wang, G.; Chen, Y.; Jiang, J. Dual stimuli-responsive wormlike micelles base on cationic azobenzene surfactant and sodium azophenol. *Colloids Surf., A* **2018**, *543*, 155–162.
- (27) Yan, Z.; Dai, C.; Zhao, M.; Sun, Y.; Zhao, G. Development, formation mechanism and performance evaluation of a reusable viscoelastic surfactant fracturing fluid. *J. Ind. Eng. Chem.* **2016**, *37*, 115–122.
- (28) Hull, K. L.; Sayed, M.; Al-Muntasheri, G. A. Recent advances in viscoelastic surfactants for improved production from hydrocarbon reservoirs. *SPE J.* **2016**, *21* (04), 1340–1357.
- (29) Gaynanova, G. A.; Valikhmetova, A. R.; Kuryashov, D. A.; Bashkirtseva, N. Y.; Zakharova, L. Y. Mixed systems based on erucyl amidopropyl betaine and nanoparticles: self-organization and rheology. *J. Surfactants Deterg.* **2015**, *18*, 965–971.
- (30) Fan, H. J.; Luo, M. L.; Jia, Z. L.; Sun, H. T. Effect of Nano-SiO<sub>2</sub> on the rheology of anionic viscoelastic solutions formed by the biodegradable surfactant fatty acid methyl ester sulfonate. *Mater. Sci. Forum* **2011**, *694*, 64–67.
- (31) Hanafy, A.; Najem, F.; Nasr-El-Din, H. A. Impact of nanoparticles shape on the VES performance for high temperature applications. In *SPE Western Regional Meeting*, 2018.
- (32) Farid Ibrahim, A.; Nasr-El-Din, H. A. An experimental study for the using of nanoparticle/VES stabilized CO<sub>2</sub> foam to improve the sweep efficiency in EOR applications. In *SPE Annual Technical Conference and Exhibition*, Dallas, Texas, USA, 2018.
- (33) Verma, A.; Chauhan, G.; Baruah, P. P.; Ojha, K. Morphology, rheology, and kinetics of nanosilica stabilized gelled foam fluid for hydraulic fracturing application. *Ind. Eng. Chem. Res.* **2018**, *57* (40), 13449–13462.
- (34) Ahmadi, M. A.; Shadizadeh, S. R. Induced effect of adding nano silica on adsorption of a natural surfactant onto sandstone rock: experimental and theoretical study. *J. Pet. Sci. Eng.* **2013**, *112*, 239–247.
- (35) Si, X.; Luo, M.; Li, M.; Ma, Y.; Huang, Y.; Pu, J. Experimental study on the stability of a novel nanocomposite-enhanced viscoelastic surfactant solution as a fracturing fluid under unconventional reservoir stimulation. *Nanomaterials* **2022**, *12* (5), 812.
- (36) Nettesheim, F.; Liberatore, M. W.; Hodgdon, T. K.; Wagner, N. J.; Kaler, E. W.; Vethamuthu, M. Influence of nanoparticle addition on the properties of wormlike micellar solutions. *Langmuir* **2008**, *24* (15), 7718–7726.
- (37) Afifi, H. R.; Mohammadi, S.; Mirzaei Derazi, A.; Mahmoudi Alemi, F. M. Enhancement of smart water-based foam characteristics by SiO<sub>2</sub> nanoparticles for EOR applications. *Colloids Surf., A* **2021**, *627*, 127143.
- (38) Afifi, H. R.; Mohammadi, S.; Derazi, A. M.; Alemi, F. M.; Hossein Abad, K. F.; Mahvelati, E. H.; Fouladi Hossein Abad, K. WITHDRAWN: A comprehensive review on critical affecting parameters on foam stability and recent advancements for foam-based EOR scenario. *J. Mol. Liq.* **2021**, 116808.
- (39) Zhao, M.; Zhang, Y.; Zou, C.; Dai, C.; Gao, M.; Li, Y.; Lv, W.; Jiang, J.; Wu, Y. Can more nanoparticles induce larger viscosities of nanoparticle-enhanced wormlike micellar system (NEWMS)? *Materials* **2017**, *10* (9), 1096.
- (40) Pletneva, V. A.; Molchanov, V. S.; Philippova, O. E. Viscoelasticity of smart fluids based on wormlike surfactant micelles and oppositely charged magnetic particles. *Langmuir* **2015**, *31* (1), 110–119.
- (41) Afifi, H. R.; Mohammadi, S.; Moradi, S.; Hamed Mahvelati, E.; Mahmoudi Alemi, F.; Ghanbarpour, O. Deriving optimal and adaptive nanoparticles-assisted foam solution for enhanced oil recovery applications: an experimental study. *J. Dispersion Sci. Technol.* **2023**, *44* (5), 819–830.
- (42) Crews, J. B.; Huang, T. Performance enhancements of viscoelastic surfactant stimulation fluids with nanoparticles. In *SPE Europec featured at EAGE Conference and Exhibition*, 2008.
- (43) Gurluk, M. R. Using nanotechnology in viscoelastic surfactant stimulation fluids. Master Thesis, Texas A&M University, 2012.
- (44) Gurluk, M. R.; Nasr-El-Din, H. A.; Crews, J. B. Enhancing the performance of viscoelastic surfactant fluids using nanoparticles. In *SPE Europec featured at EAGE Conference and Exhibition*, 2013.
- (45) Destefani, T. A.; Lavandoski Onaga, G.; de Farias, M. A.; Percebom, A. M.; Sabadini, E. Stabilization of spherical nanoparticles of iron (III) hydroxides in aqueous solution by wormlike micelles. *J. Colloid Interface Sci.* **2018**, *513*, 527–535.
- (46) Sambasivam, A.; Dhakal, S.; Sureshkumar, R. Structure and rheology of self-assembled aqueous suspensions of nanoparticles and wormlike micelles. *Mol. Simul.* **2018**, *44* (6), 485–493.
- (47) Patel, M. C.; Ayoub, M. A.; Hassan, A. M.; Idress, M. B. A novel ZnO nanoparticles enhanced surfactant based viscoelastic fluid systems for fracturing under high temperature and high shear rate conditions: Synthesis, rheometric analysis, and fluid model derivation. *Polymers* **2022**, *14* (19), 4023.
- (48) Liu, Z.; Wang, Q.; Gao, M.; Luo, W.; Cai, H. Study of rheological property and flow behavior for nanoparticles enhanced VES system in porous media. *Front. Energy Res.* **2021**, *9*, 598177.
- (49) Zhu, J.; Yang, Z.; Li, X.; Hou, L.; Xie, S. Experimental study on the microscopic characteristics of foams stabilized by viscoelastic surfactant and nanoparticles. *Colloids Surf., A* **2019**, *572*, 88–96.
- (50) Yekeen, N.; Padmanabhan, E.; Idris, A. K. Synergistic effects of nanoparticles and surfactants on n-decane-water interfacial tension and bulk foam stability at high temperature. *J. Pet. Sci. Eng.* **2019**, *179*, 814–830.
- (51) Aggarwal, A.; Agarwalm, S.; Sharmam, S. Viscoelastic surfactants based stimulation fluids with added nanocrystals and self-suspending proppants for HPHT applications. In *Abu Dhabi International Petroleum Exhibition and Conference*, 2014.
- (52) Helgeson, M. E.; Hodgdon, T. K.; Kaler, E. W.; Wagner, N. J.; Vethamuthu, M.; Ananthapadmanabhan, K. Formation and rheology of viscoelastic “double networks” in wormlike micelle-nanoparticle mixtures. *Langmuir* **2010**, *26* (11), 8049–8060.
- (53) Fanzatovich, I. I.; Aleksandrovich, K. D.; Rinatovich, I. A.; Yur'evna, B. N.; Yarullova, Z. L.; Valerevich, Z. S.; Rashidovna, A. M.; Evgenevna, K. N. Supramolecular system based on cylindrical micelles of anionic surfactant and silica nanoparticles. *Colloids Surf., A* **2016**, *507*, 255–260.
- (54) Fan, Q.; Li, W.; Zhang, Y.; Fan, W.; Li, X.; Dong, J. Nanoparticles induced micellar growth in sodium oleate wormlike micelles solutions. *Colloid Polym. Sci.* **2015**, *293*, 2507–2513.
- (55) Oseh, J. O.; Norddin, M. N. A. M.; Ismail, I.; Duru, U. I.; Gbadamosi, A. O.; Agi, A.; Nguouangna, E. N.; Blkooor, S. O.; Yahya, M. N.; Risal, A. R. Rheological and filtration control performance of water-based drilling muds at different temperatures and salt

contaminants using surfactant-assisted novel nanohydroxyapatite. *Geo. Sci. Eng.* **2023**, *228*, 211994.

(56) Najjar, P. A.; Mohammadi, S.; Mirzayi, B.; Mahmoudi Alemi, F.; Ghanbarpour, O. A mechanistic study of asphaltene formation and aggregation in presence of metallic-based nanoparticles. *Geo. Sci. Eng.* **2024**, *234*, 212637.

(57) Mahmoudi Alemi, F.; Mousavi Dehghani, S. A.; Rashidi, A.; Hosseinpour, N.; Mohammadi, S. Potential application of Fe<sub>2</sub>O<sub>3</sub> and functionalized SiO<sub>2</sub> nanoparticles for inhibiting asphaltene precipitation in live oil at reservoir conditions. *Energy Fuels* **2021**, *35*, 5908–5924.

(58) Wayan Sutapa, I.; Wahid Wahab, A.; Taba, P.; La Nafie, N. Synthesis and structural profile analysis of the MgO nanoparticles produced through the sol-gel method followed by annealing process. *Orient. J. Chem.* **2018**, *34*, 1016–1025.

(59) Lunkenheimer, K.; Malysa, K. Simple and generally applicable method of determination and evaluation of foam properties. *J. Surfactants Deterg.* **2003**, *6*, 69–74.

(60) Belhaj, A.; AlQuraishi, A.; Al-Mahdy, O. Foamability and foam stability of several surfactants solutions: the role of screening and flooding. In *SPE Kingdom of Saudi Arabia Annual Technical Symposium and Exhibition*, 2014.

(61) Díaz-Díez, M.; Gómez-Serrano, V.; Fernández González, C.; Cuerda-Correa, E. M.; Macías-García, A. Porous texture of activated carbons prepared by phosphoric acid activation of woods. *Appl. Surf. Sci.* **2004**, *238*, 309–313.

(62) Raj, K. A.; Balikram, A.; Ojha, K. Impact assessment of nanoparticles on microstructure and rheological behaviour of VES fracturing fluid formulated with mixed surfactant system. *J. Mol. Liq.* **2022**, *345* (345), 118241.